Optical Properties of SiO2 – TiO2 – La2O3 – Na2O – Y2O3 glasses and A novel process of preparing the parent glass-ceramics

A. F. Abd El-Rehim
King Khaled University
E. A Abdel Wahab
Al-Azhar University
M. M. Abou Halaka
Al-Azhar University
Kh. S. shaaban (khamies1078@yahoo.com)
Al-Azhar University https://orcid.org/0000-0002-5969-3089

Original Research

Keywords: Yttrium, UV, Glass-ceramics, XRD, SEM

Posted Date: February 3rd, 2021

DOI: https://doi.org/10.21203/rs.3.rs-187779/v1

Version of Record: A version of this preprint was published at Silicon on February 26th, 2021. See the published version at https://doi.org/10.1007/s12633-021-01002-w.

Optical Properties of $SiO_2 – TiO_2 – La_2O_3 – Na_2O – Y_2O_3$ glasses and A novel process of preparing the parent glass-ceramics

A.F. Abd El-Rehim [1,2], E. A. Abdel Wahab[3], M. M. Abou Halaka[3], Kh. S. Shaaban[4]

[1] Physics Department, Faculty of Science, King Khalid University, P.O. Box 9004, Abha 61413, Saudi Arabia.
[2] Physics Department, Faculty of Education, Ain Shams University, P.O. Box 5101, Heliopolis 11771, Roxy, Cairo, Egypt
[3]Physics Department, Faculty of Science, Assiut University, P.O. 71524, Assiut, Egypt
[4]Chemistry Department, Faculty of Science, Al-Azhar University, P.O. 71524, Assiut, Egypt

Abstract:

Quaternary glasses with the composition $50SiO_2 – 25TiO_2 – 5La_2O_3 – (20\text{-}x)\ Na_2O – xY_2O_3$ where $x: (0 \leq x \geq 10)$ were synthesized using the melt-quench technique. XRD examined the nature of prepared glasses. UV-spectroscopic of investigated glass system studied at room temperature. Both optical bandgap and refractive index of the present glass have been increased. The polarizability and basicity were determined. Thermal parameter values increased as Y_2O_3 increased. Under controlling heat, the glass-ceramic were prepared and confirmed using XRD. Glass-ceramics are examined using SEM to evaluate a microstructure. Ultrasonic velocities and elastic-moduli of glass-ceramic samples are increased because of the increase in internal energy. The role of Y_2O_3 modifier in the glass system is clearly demonstrated. Y_2O_3 also works as an excellent nucleating agent that can induce crystallizations, supporting in the creation of the sub-phase of glass-ceramics.

Keywords: Yttrium, UV, Glass-ceramics, XRD, SEM.

Corresponding Author: khamies1078@yahoo.com

1-Introduction

Glasses containing transition metals oxides attract the attention of several researchers for excellent infrared transmission compared with the conventional glasses. It makes an ideal candidate for various applications such as infrared transmission components, ultra-fast optical

switches, and photonic devices [1-3]. Silicate glasses containing transition metal ions exhibit unique and versatile structural properties in physical and spectral (optical & FTIR) studies. In recent years, the studies on transition metal ions containing glasses have been increased due to their admirable improvements in semiconducting properties and optoelectronic electronic devices. The abundance of multiple valance states of transition metal ions which arises from unfilled d- orbitals made them a potential candidate for extending their applicability in electrical memory switching, photo-conducting, solid-state batteries, and electronic devices [4]. Transition metal ions containing glass are considered semiconducting substances. Nowadays The glasses are considered potential applicants for electronic, mechanical, and optical [4].

TiO_2 containing glasses show remarkable properties like low phonon frequency, high dielectric, non-linear optical, electric, and magnetic. Under these characteristics glass doped TiO_2 has extend applications in the field of optics, photonics, optoelectronics, and telecommunication devices. In glasses, usually TiO_2, are intermediate, crystallizing agents and it may be observed in the Ti^{4+} and involved in the structural units of TiO_4, TiO_6 and TiO_5 [5-10].

The incorporation of Y_2O_3 into sodium-silicate glasses causes the replacement of weak Si-O-Na bonds with strong Si-O-Y bonds lead to enhances the thermal, optical & chemical stability of host glasses. The introduction of Y_2O_3 into the glass network enhanced the optical and physical properties of the glass [11]. Glasses containing rare-earth ions have several optical and photonic applications available [12-19]. It is highly possible for UV optics and solid-state batteries applications because of the good ionic conductivity of these glasses [12-19]. Considering the importance of sodium titanium silicate glasses in scientific and technological, characteristics like ionic conductivity in power generation glasses modified with various oxides are strongly required [20-21]. In contrast, the incorporation of transitional or rare earth oxides into sodium titanium silicate glass structures are enhanced optical, electrical, thermal,

mechanical and radiation protection characteristics [22-25]. Glasses containing rare-earth ions have attracted a great deal of interest because of their benefits [26-31]. Intermediate oxides such as Y_2O_3 can act either as a glass modifier or former, depending on their concentration in the glass matrix. Y_2O_3 enhances the host glass matrix's physical structure and mechanical strength. [32-38]. The existence of Y_2O_3 enhances the capacity to form glass and reduces devitrification. The existence of TiO_2 and Y_2O_3 impacts UV-spectroscopic in glass systems. These glasses possess lower photon energy and higher refractive index than other glasses. Scientifically and technologically, the recent innovation of titanium silicate glasses containing Y_2O_3 and La_2O_3 is very significant.

In the 1950s, Stookey and Kingery [39] discovered the first glass-ceramic that could be manufactured industrially by adding the nucleating agent TiO_2 to control the devitrification of glass. Even at the end of the nineteenth century, Mc. Millan used crystallization [40]. After Stookey's discovery of the controlled nucleation and crystallization of glass-ceramics, several studies on sintered glass-ceramics were published [41-42]. Glass-ceramics are polycrystalline materials formed by heat treatment of glasses of appropriate compositions. Crystallization is an important topic in glass science as well as in glass technology. The crystallization behavior and the final properties of glass ceramics parts are mainly affected by the configuration of the parental glass, the nucleating system, and the crystallization conditions. In comparison to those of the parent glass, the mechanical properties of glass-ceramics are better. Glass-ceramics can also, exert other unusual characteristics that are valuable for purposes, as shown by the incredibly small thermal expansion coefficient, which is therefore acceptable for thermal shock-resistant implementations. The goal of our article is preparing of lanthanum titanium silicate glasses containing yttrium and investigating their structural and optical properties.

2. Experimental processes and techniques.

The glasses in this study were synthesized from $50SiO_2 – 25TiO_2 – 5La_2O_3 – (20\text{-}x)$ $Na_2O – xY_2O_3$ in platinum crucible using the melt-quench technique method where x: $(0 \leq x \geq 10)$ mol %. The starting materials are SiO_2, Na_2CO_3, La_2O_3, Y_2O_3 and TiO_2 with high purity. All chemicals used for the glass preparation obtained from Sigma-Aldrich. The starting materials were mixed by grinding the mixture repeatedly to obtain a fine powder. Firstly, the starting materials have been heated to 450°C for 4 h to eliminate H_2O, and CO_2. The temperature has been raised to 1200°C for 30 min. The glasses were annealed at 450°C for 2 h to relieve the internal stresses and allowed to cool gradually to room temperature. The weight losses were found to be less than 1%.

The amorphous state of the glasses and glass-ceramics were checked using X-ray diffraction. A Philips X-ray diffractometer PW/1710 with Ni-filtered Cu-Kα radiation (λ = 1.542 Å) powered at 40 kV and 30 mA was used. UV-spectroscopic of investigated glass system is studied by spectrophotometer (type JASCO V-670). Archimedes principle describes the density as the following relation: $\rho = \rho_0 \left(\frac{C}{C-C_1}\right)$, the weight of samples in air and liquid is C and C1 respectively, the density of glass-ceramic sample is ρ, and toluene is ρ_0 (0.865) g/cm^3. DTA-50 (type Shimadzu) used for the thermal investigation. By heating the specimen at specified temperatures on two steps, first, at 500 °C, the glass-ceramics are produced, the sconed is 1 hour at T_c °C, the crystal growth. A pulse-echo method is used to study mechanical measurements for glass-ceramics by (KARL DEUTSCH Echograph model-1085). The model (JEM-100 CX 11 JAPAN), a scanning microscope (SEM), has been used to examine the morphology of investigated glass-ceramic.

3. Results and Discussions

3.1 XRD Observations

Fig.1. shows the X-ray results of the studied glasses. These diffractograms show no discrete lines, no sharp peaks, and indicate that glass samples have a high degree of glassy state. The slight shift in the hump at (15 - 30) 2θ° values with respect to Y_2O_3 concentration can be related to the decrease in the bond length and to the higher coordination number with oxygens.

3.2 UV-Visible absorption spectra

UV-Vis-NIR absorption spectroscopy is a completely beneficial approach to characterize the optical of different substances which include thin films, filters, pigments, glass, and glass ceramics. Optical absorption spectra of various Y_2O_3 co-doped glasses in wavelength range 200 – 2700 nm were investigated. Fig.**2** exemplifies the absorbance (A) and transmittance (T) of glass samples. Fig. **3** exemplifies the reflectance (R) of these glasses. There have indications of increasing the absorption coefficient as Fig. **4**. Therefore, Y_2O_3 is accounted as BO development [43]. The absorption coefficient $\propto$ was calculated by: $\propto(\lambda) = \frac{1}{x}\ln\left(\frac{1-R}{T}\right)$, Where *x* is sample thickness.

3.2.1 Optical band gap E_{opt}

Absorption spectra of glasses in the ultraviolet and visible regions have been used to calculate optical band gap. Optical band gap is determined by $(\alpha.h\nu)^{1/2} = B(h\nu - E_{opt.})$ where E_{opt} is optical band gap, B is an energy independent constant and $h\nu$ is photon energy. By plotting the $(\alpha.h\nu)^{1/2}$ versus $h\nu$ as Fig.5. The intercept of $\sqrt{\alpha h\nu}$ versus hν at $\sqrt{\alpha h\nu} = 0$ denoted the value of E_{opt}. It was noted with increasing Y_2O_3 content the energy gap increases as in table 2. This increase can be explained as oxygen bridges (BO) are generated that bind energized electrons more strongly than non-bridging oxygen (NBO). Also, this increasing of E_{opt} may be due to change in composition of glass matrix and increase the interconnection.

3.2.2 Refractive index (n)

According to the theory of reflectivity of light, the refractive index (n) values obtained as a function of the reflectance (R) and the extinction coefficient (k) as: $n = \frac{(1-R)^2+k^2}{(1+R)^2+k^2}$,where k values have been determined using the relation ($k = \alpha\lambda/4\pi$). According to the Lorentz–Lorenz equation, the density of the material affects the refractive index in a direct proportion. Thus, the increase in the values of the refractive index is ascribed to the increase in density of the glass. The refractive index of studied glasses shown in Fig.**6**. The refractive index of the studied glasses increases with increasing of the wavelength and with increasing of Y_2O_3 content.

3.2.3 Dispersion parameters

Molar polarization, and polarizability of glasses have been projected as $R_m = \langle n^2-1|n^2+2\rangle Vm$, $\propto_m = (3|4\pi N)R_m$, and $\propto_0^{2-} = \frac{[\frac{Vm}{2.52}\left(\frac{n^2-1}{n^2+2}\right)-\Sigma\propto_{cat}]}{N_o^{2-}}$ [44-48] where $Vm\ is\ molar\ volume$, n is refractive index, N Avogadro number, and No number of oxygen atom. The optical basicity of the samples prepared was linked to polarization; $\Lambda = 1.67\left(1-\frac{1}{\propto_0^{2-}}\right)$. Figures **7**,**8**&**9** present the Molar Polarizability $\propto_m$, polarizabilities and optical basicity respectively of prepared samples, it was observed the same trend of refractive index with increasing concentrations of Y_2O_3 [45–48].

The molar refractivity depends on $E_{opt.}$ $R_m = Vm\left(1-\sqrt{Eopt./20}\right)$ and molar polarizability ($\propto_m$). Reflection loss $R_L = \left(\frac{R_m}{Vm}\right)$. These values of ($R_m$) ($\propto_m$) and ($R_L$) decrease with yttrium because of the decrease in the molar volume are presented in Table **2**. The criterion for metallization is predicted as $M = 1-\frac{R_m}{Vm}$, the metallization value rises with Y^{+3}. The electronegativity (χ) is predicted as $\chi = 0.2688E_{opt.}$. where $E_{opt.}$ bandgap. Thus, with Y^{+3} increasing, the electronegativity (χ) values increase. The electron polarizability is predicted as, $\propto^\circ = -0.9\,\chi + 3.5$ and optical basicity $\wedge = -0.5\chi + 1.7$. $\propto^\circ$ and $\wedge$ have the inverse trend

of (χ) thus, with Y^{+3} increase $\propto$ ° and $\wedge$ decrease. This explanation is linked to the value of the optical basicity of Y_2O_3 (0.99) and Na_2O s (1.15) [47-48]. Table **2** shows the variation of these values.

3.3 Thermal analysis

DTA-thermograms are the best way to show thermal properties. The first thermal attribute is the transition temperature of samples T_g, while the following thermal property consists of T_c and T_p crystallization and peak temperatures. DTA-thermograms of glasses are presented in Fig. **10**. It is observed that these parameters have been increased as the Y_2O_3 increases. This is related to increase in the connection of the glass structure. According to these parameters, the glass-ceramics have been prepared. The estimated thermal stability values as: $\Delta T = (Tc - Tg)$, $Hg = \frac{\Delta T}{Tg}$,and $S = (Tp - Tc)\ \frac{\Delta T}{Tg}$ are listed in Table **3.**

It indicated that, the increasing with increasing of Y_2O_3 content is due to the transformation of Si–O−Na into Si –O−Y, and Na−O bond strength is (20 KCal/mol) is much lower than Y−O (50KCal/mol) **[**49**]**. This behavior is linked to the modification of the coordination number with increasing Y_2O_3, the growth in average constant force and cross-link density. As Y_2O_3 increases at expense of Na_2O, the molar volume decreases and the density increases, making the glass structure more compact.

3.4 XRD and SEM analysis for consistent ceramic-glass

Glass- ceramics have been investigated using XRD for further analysis, as seen in the Fig. 11. The XRD pattern of G1 and G6 are similar, as noticeable from the Fig. 11, excluding that diffraction peaks are stronger. High transparency, uniform color, and good chemical and mechanical properties were exhibited due to an increasing the content of Y_2O_3. The network of sodium silicate units could be broken by Y_2O_3 and act as a glass stabilizer, thereby increasing

chemical structure and mechanical hardness. Because the transformation of Si– O– Na into Si – O–Y, and Na–O bond strength is (20KCal/mol) is much lower than Y –O (50KCal/mol).

The strongest phases are Lanthanum Titanium Silicate, $La_2(Ti_2SiO_9)$, card No. 01-082-1490, Lanthanum Titanium Silicate Oxide, $La_4Ti\ (Si_2O_7)_2\ (Ti_8O_{16})$ card No. 01-079-2299 and less strongly phase Lanthanum Titanium Silicate Oxide $La_4Ti_5\ (Si_2O_7)_2O_8$ card No. 01-083-023. New phases have emerged through the increase in yttrium oxide Lanthanum Yttrium Titanium Oxide $La_{0.5}Y_{0.5}TiO_3$ card No. 01-073-0070 and Yttrium Titanium Silicon Oxide (Trimounsite-(Y)) $Y_2Ti_2SiO_9$ card No. 00-046-1375. The microcracks had been easily obtained during the recrystallization process based on differences in the coefficients of thermal expansion between the phases of yttrium and the impeccable standards phase, helping to make the glass-ceramic much harder.

Glass-ceramics had been examined using SEM, as seen in Figs, **12**A&12B to evaluate a microstructure. The size of the crystal is listed in Table **4&5**. SEM photograph of selected glass-ceramic samples. It is indicated that uniform distributions in the glass composition. Figure 12a show the micrographically (G1). It is indicated a nearly unchanging on the surface. Lanthanum Titanium Silicate was crystallized in occasional crystalline texture that includes comparatively large interstitial pores reflecting the remaining glassy matrix. Figure 12b illustrations the micrographically (G6). It is indicated that uniform distributions in the glass composition [50]. With the increase of Y_2O_3 content, the possibility of crystallization is increased, and a glass sub-phase has been created to increase the internal energy.

3.5 Mechanical Properties of Glass-Ceramics

Figures 13 & Tables **6** represented sound velocities of glass-ceramics. This found that Y_2O_3 increases those velocities. Due to increase in density, bonding strength, and cross-link density. The increase in sound velocities because the increase in the internal energy.

To determine elastic-moduli as, $L = \rho v_l^2$, $G = \rho v_s^2$, $Y = (1+\sigma)2G$, and, $K = L - \left(\frac{4}{3}\right)G$. Elastic-moduli of glass-ceramic have been estimated and represented in Figure **14** and Table **6**. It indicated that, these moduli increasing with the Y_2O_3 increase. Tis due to transformation of Si −O−Na into Si −O−Y, and Na −O bond strength is (20 KCal/mol) is much lower than B −O (50 KCal/mol).

Poisson's ratio is projected as $\sigma = \frac{1}{2} - \left(\frac{1}{7.2^* Vi}\right)$, Micro-hardness is projected as $H = \frac{(1-2\sigma)Y}{6(1+\sigma)}$, Thermal Expansion ($\alpha_P$), $\alpha_{P\,=23.2\,(v_L-0.57457)}$ and acoustic impedance (Z). All these parameters are shown in Table **6** and they increased as the yttrium content increase because of the role of a Y_2O_3 modifier in the glass system is clearly demonstrated.

4. Conclusions

Quaternary glasses with the composition of $50SiO_2 – 25TiO_2 – 5La_2O_3 – (20\text{-}x)\,Na_2O – xY_2O_3$ have been manufactured using conventional melt-quenching methods. The optical, thermal, crystallization, and mechanical variables have been examined for these glasses. The findings showed the following objects:

1- XRD measurements established the amorphous nature of glasses.

2- Optical absorption was quantified to understand the optical characteristics of the prepared glasses.

3- With increasing Y_2O_3 content the energy gap increases. This grow can be explained as oxygen bridges (BO) are generated that bind energized electrons more strongly than non-bridging oxygen (NBO).

4- Refractive index of investigated glasses are increases as density increase.

5- Molar polarization, polarizability, and optical basicity of these glasses having the same trend of refractive index with concentration of Y_2O_3 increased.

6- Metallization of these glasses were enhanced because of increment of TiO_2.

7- Thermal stability of these glasses was increased as the Y_2O_3 increases. These increases related to increase in the connection of the glass structure.

8- Under controlling heat, the glass-ceramic was prepared and investigated by XRD, SEM, and mechanical properties.

9- XRD results showed all the expected phases due to the crystallization process.

10- SEM photograph of selected glass-ceramic samples indicated that uniform distributions in the glass composition.

11- Ultrasonic velocities and elastic-modules of glass-ceramic samples are increased because of increase in internal energy.

Acknowledgment

The authors extend their appreciation to the Deanship of Scientific Research at King Khalid University for funding this work through research groups program under grant number R.G.P. 2/93/41.

Author contributions: Kh. S. Shaaban: performing XRD, UV measurements and analysis, Writing-review, writing manuscript, Methodology, Software, and writing – discussion.

A.F. Abd El-Rehim: Writing-review, writing – discussion and editing manuscript.

E. A. Abdel Wahab: Writing-review, writing – discussion and editing manuscript.

M. M. Abou Halaka: Writing-review, writing – discussion and editing manuscript.

Availability of data and material: My manuscript and associated personal data will be shared with Research Square for the delivery of the author dashboard.

Compliance with ethical standards: The manuscript has not been published elsewhere and that it has not been submitted simultaneously for publication elsewhere.

Conflict of interest: The authors declare that they have no conflict of interest.

Declaration of Competing Interest: The authors declare that they have no known competing financial interests or personal relationships that could have appeared to influence the work reported in this paper.

Funding statement: There are currently no Funding Sources in the list

Consent to participate: The authors consent to participate.

Consent for Publication: The authors consent for publication.

References

[1] El-Damrawi, G., Abdelghany, A.M., Hassan, A.K. et al. (2020) Effect of BO_4 and FeO_4 Structural Units on Conduction Mechanism of Iron Borosilicate Glasses. Silicon. https://doi.org/10.1007/s12633-020-00694-w

[2] El-Damrawi G, Abdelghany AM, Oraby AH, Madshal MA (2020) Structural and optical absorption studies on Cr_2O_3 doped SrO-P_2O5 glasses. Spectrochimica Acta Part A: Molecular and Biomolecular Spectroscopy **228**:117840https://doi.org/10.1016/j.saa.2019.117840

[3] Livage, J., Jolivet, J. P., & Tronc, E. (1990). Electronic properties of mixed valence oxide gels. Journal of Non-Crystalline Solids, **121**(1-3), 35–39. doi:10.1016/0022-3093(90)90100-z

[4] Ghosh, A. (1988). Memory switching in bismuth-vanadate glasses. Journal of Applied Physics, **64**(5), 2652–2655. doi:10.1063/1.341605

[5] Reddy, A.P., Rao, P.N., Reddy, M.C.S. et al. (2020) Second harmonic generation and spectroscopic characteristics of TiO_2 doped Li_2O–Al_2O_3–B_2O_3 glass matrix. Appl. Phys. A 126, 689. https://doi.org/10.1007/s00339-020-03879-7

[6] Shaaban, K.S., Wahab, E.A.A., Shaaban, E.R. et al. (2020). Electronic Polarizability, Optical Basicity, Thermal, Mechanical and Optical Investigations of ($65B_2O_3$–$30Li_2O$–$5Al_2O_3$) Glasses Doped with Titanate. Journal of Elec Materi 49, 2040–2049.
https://doi.org/10.1007/s11664-019-07889-x

[7] Shaaban, K.S., Koubisy, M.S.I., Zahran, H.Y. et al. (2020). Spectroscopic Properties, Electronic Polarizability, and Optical Basicity of Titanium–Cadmium Tellurite Glasses Doped with Different Amounts of Lanthanum. J Inorg Organomet Polym. https://doi.org/10.1007/s10904-020-01640-4

[8] Shaaban, K.S., Yousef, E.S., Mahmoud, S.A. *et al.* (2020). Mechanical, Structural and Crystallization Properties in Titanate Doped Phosphate Glasses. J Inorg Organomet. Polym https://doi.org/10.1007/s10904-020-01574-x

[9] Wahab, E. A. A., & Shaaban, K. S. (2018). Effects of SnO_2 on spectroscopic properties of borosilicate glasses before and after plasma treatment and its mechanical properties. Materials Research Express, 5(2), 025207, doi:10.1088/2053-1591/aaaee8

[10] Hussain, I., Barimah, E. K., Iqbal, Y., Jose, G., & Muhammad, R. (2019). Thermal, Mechanical and Optical Properties of TiO_2-doped Sodium Silicate Glass-Ceramics. Transactions of the Indian Ceramic Society, 1–6. doi:10.1080/0371750x.2019.1626287

[11] Shaaban, K.S., Abo-Naf, S.M. & Hassouna, M.E.M. (2019). Physical and Structural Properties of Lithium Borate Glasses Containing MoO_3. Silicon **11,** 2421–2428 https://doi.org/10.1007/s12633-016-9519-4

[12] Abdel Wahab, E.A., Shaaban, K.S., Elsaman, R. *et al.* (2019). Radiation shielding, and physical properties of lead borate glass doped ZrO_2 nanoparticles. Appl. Phys. A **125,** 869 https://doi.org/10.1007/s00339-019-3166-8

[13] Nayak, Manjunath T.; Desa, J.A. Erwin; Babu, P.D. (2018). Magnetic and spectroscopic studies of an iron lithium calcium silicate glass and ceramic. Journal of Non-Crystalline Solids,484,1-7, doi: 10.1016/j.jnoncrysol.2017.12.050

[14] Nayak, Manjunath T.; Desa, J.A. Erwin (2018). Roles of iron and lithium in silicate glasses by Raman spectroscopy. Journal of Raman Spectroscopy, (), –. doi:10.1002/jrs.5397

[15] Nayak, Manjunath T.; Desa, J.A. Erwin; Reddy, V. Raghvendra; Nayak, C.; Bhattacharyya, D.; Jha, S.N. (2019). Structures of silicate glasses with varying sodium and fixed iron contents. Journal of Non-Crystalline Solids, 509, 42–47. doi: 10.1016/j.jnoncrysol.2019.01.009

[16] Abd-Allah, W.M., Saudi, H.A., Shaaban, K.S. *et al.* (2019), Investigation of structural and radiation shielding properties of $40B_2O_3$–30PbO–(30-*x*) BaO-*x* ZnO glass system. Appl. Phys. A **125,** 275 https://doi.org/10.1007/s00339-019-2574-0

[17] Shaaban, K. S., Abo-naf S. M., Abd Elnaeim, A. M., & Hassouna, M. E. M. (2017). Studying effect of MoO_3 on elastic and crystallization behavior of lithium diborate glasses. Appl. Phys. A, 123(6), doi:10.1007/s00339-017-1052-9

[16] Algradee, M. A., Sultan, M., Samir, O. M., & Alwany, A. E. B. (2017). Electronic polarizability, optical basicity and interaction parameter for Nd_2O_3 doped lithium–zinc–phosphate glasses. Applied Physics A, 123(8). doi:10.1007/s00339-017-1136-6

[17] Shaaban, K., Abdel Wahab, E.A., El-Maaref, A.A. *et al.* (2020). Judd–Ofelt analysis and physical properties of erbium modified cadmium lithium gadolinium silicate glasses. J Mater Sci: Mater Electron **31,** 4986–4996 https://doi.org/10.1007/s10854-020-03065-8

[18] Shaaban, K.S., Yousef, E.S., Abdel Wahab, E.A. *et al.* (2020). Investigation of Crystallization and Mechanical Characteristics of Glass and Glass-Ceramic with the Compositions $x$$Fe_2O_3-35SiO_2-35B_2O_3-10Al_2O_3$-(20−$x$) Na_2O. J. of Materi Eng and Perform. https://doi.org/10.1007/s11665-020-04969-6

[19] El-Maaref, A. A., Shimaa Badr, Shaaban, K. S., Wahab, E. A. A., & ElOkr, M. M. (2019), Optical Properties and Radiative Rates of Nd^{3+} Doped Zinc-Sodium Phosphate Glasses. Journal of Rare Earths 37, 3, 253-259 doi: 10.1016/j.jre.2018.06.006

[20] Shaaban, K.S., Wahab, E.A.A., Shaaban, E.R. et al. (2020). Electronic polarizability, optical basicity and mechanical properties of aluminum lead phosphate glasses. Opt Quant Electron **52,** 125 https://doi.org/10.1007/s11082-020-2191-3

[21] Shaaban, K.S., Zahran, H.Y., Yahia, I.S. et al. (2020), Mechanical and radiation-shielding properties of B_2O_3–P_2O_5–Li_2O–MoO_3 glasses. Appl. Phys. A 126, (10), 804. https://doi.org/10.1007/s00339-020-03982-9

[22] Saudi, H.A., Abd-Allah, W.M. & Shaaban, K.S. (2020). Investigation of gamma and neutron shielding parameters for borosilicate glasses doped europium oxide for the

immobilization of radioactive waste. J Mater Sci: Mater Electron 31(9), 6963-6976, https://doi.org/10.1007/s10854-020-03261-6

[23] Nayak, Manjunath T.; Desa, J.A. Erwin; Reddy, V. Raghvendra; Nayak, C.; Bhattacharyya, D.; Jha, S.N. (2019). Structural studies of potassium silicate glasses with fixed iron content and their relation to similar alkali silicates. Journal of Non-Crystalline Solids, 518(), 85–91. doi: 10.1016/j.jnoncrysol.2019.04.025

[24] Nayak, Manjunath T.; Desa, J. A. Erwin; Babu, P. D. (2018). AIP Conference Proceedings [Author(s) DAE SOLID STATE PHYSICS SYMPOSIUM 2017 - Mumbai, India (26–30 December 2017)] - Magnetic properties of Fe–Nd silica glass ceramics. , 1942(1), 070006–. doi:10.1063/1.5028804

[25] Nayak, Manjunath T.; Desa, J. A. Erwin; Babu, P. D. (2019). AIP Conference Proceedings [AIP Publishing DAE SOLID STATE PHYSICS SYMPOSIUM 2018 - Hisar, Haryana, India (18–22 December 2018)] DAE SOLID STATE PHYSICS SYMPOSIUM 2018 - Effect of iron and sodium inclusion on some properties of silicate glass. 2115(1), 030224–. doi:10.1063/1.5113063

[26] E.A. Abdel Wahab, M.S.I. Koubisy, M.I. Sayyed, K.A. Mahmoud, A.F. Zatsepin, Sayed A. Makhlouf, Shaaban, Kh.S. (2020), Novel borosilicate glass system: $Na_2B_4O_7$-SiO2-MnO_2 Synthesis, average electronics polarizability, optical basicity, and gamma-ray shielding features, Journal of Non-Crystalline Solids, https://doi.org/10.1016/j.jnoncrysol.2020.120509

[27] El-Sharkawy, R. M., Shaaban, K. S., Elsaman, R., Allam, E. A., El-Taher, A., & Mahmoud, M. E. (2020). Investigation of mechanical and radiation shielding characteristics of novel glass systems with the composition xNiO-20ZnO-60B_2O_3-(20-x) CdO based on nano metal oxides. Journal of Non-Crystalline Solids, 528,119754 doi: 10.1016/j.jnoncrysol.2019.119754

[28] Shaaban, K. S., El Sayed Yousef. (2020), Optical properties of Bi_2O_3 doped boro tellurite glasses and glass ceramics. Optik - International Journal for Light and Electron Optics 203, 163976. https://doi.org/10.1016/j.ijleo.2019.163976

[29] El-Rehim, A.F.A., Shaaban, K.S., Zahran, H.Y. et al. (2020). Structural and Mechanical Properties of Lithium Bismuth Borate Glasses Containing Molybdenum (LBBM) Together with their Glass–Ceramics. J Inorg Organomet Polym https://doi.org/10.1007/s10904-020-01708-1

[30] El-Maaref, A. A., Wahab, E. A. A., Shaaban, K. S., Abdelawwad, M., Koubisy, M. S. I., Börcsök, J., & Yousef, E. S. (2020). Visible and mid-infrared spectral emissions and radiative rates calculations of Tm^{3+} doped BBLC glass. Spectrochimica Acta Part A: Molecular and Biomolecular Spectroscopy, 118774. doi: 10.1016/j.saa.2020.118774

[31] Gedam, R.S., Ramteke, D.D. (2012). Synthesis and Characterization of Lithium Borate Glasses Containing La_2O_3. Trans Indian Inst Met 65, 31–35. https://doi.org/10.1007/s12666-011-0107-4

[32] Kaewjaeng, S., Kothan, S., Chaiphaksa, W., Chanthima, N., Raja Ramakrishna, R., Kim, H. J., & Kaewkhao, J. (2019), High transparency La_2O_3-CaO-B_2O_3-SiO_2 glass for diagnosis x-rays shielding material application, Radiation Physics and Chemistry, 160,41-47, 10.1016/j.radphyschem.2019.03.018

[33] Rajaramakrishna, R., Karuthedath, S., Anavekar, R. V., & Jain, H. (2012). Nonlinear optical studies of lead lanthanum borate glass doped with Au nanoparticles. Journal of Non-Crystalline Solids, 358(14), 1667–1672, doi: 10.1016/j.jnoncrysol.2012.04.031

[33] Fayad, A.M., Abd-Allah, W.M. & Moustafa, F.A. (2018). Effect of Gamma Irradiation on Structural and Optical Investigations of Borosilicate Glass Doped Yttrium Oxide. Silicon 10, 799–809.https://doi.org/10.1007/s12633-016-9533-6

[35] Singh, K., Gupta, N. & Pandey, O.P. (2007). Effect of Y_2O_3 on the crystallization behavior of SiO_2–MgO–B_2O_3–Al_2O_3 glasses. J Mater Sci 42, 6426–6432 https://doi.org/10.1007/s10853-006-1188-z

[36] Kumar V, Pandey OP, Singh K, (2010). Effect of A_2O_3 (A = La, Y, Cr, Al) on thermal and crystallization kinetics of borosilicate glass sealants for solid oxide fuel cells Glasses. Ceram Int 36 (5): 1621- 1626, https://doi.org/10.1016/j.ceramint.2010.02.040

[37] Singh S, Kalia G, Singh K, (2015). Effect of intermediate oxide (Y_2O_3) on thermal, structural and optical properties of lithium borosilicate glasses. Mol Struct 1086:239–245, https://doi.org/10.1016/j.molstruc.2015.01.031

[38] E.A. Abdel Wahab, A.A. El-Maaref, Kh.S. Shaaban, J. Börcsök, M. Abdelawwad, (2020), Lithium cadmium phosphate glasses doped Sm^{3+} as a host material for near-IR laser applications, Optical Materials,110638, https://doi.org/10.1016/j.optmat.2020.110638.

[39] Stookey, S. D. and Kingery, W. D. Ceramic Fabrication Processes. John Wiley and Sons, Inc. New York. 1960

[40] McMillan, P.W., Glass-Ceramics. 2nd ed. Non-Metallic Solids, ed. J.P. Roberts. Vol. 1. London: Academic Press Inc. (London) Ltd. (1979).

[41] Hölland, W., Beall, G., Glass-Ceramic Technology, The American Ceramic Society, Westerville, OH, (2002).

[42] Strnad, Z., Glass-Ceramic Materials. Elsevier, Amsterdam (1986).

[43] Abdel Wahab, E.A., Shaaban, K.S. & Yousef, E.S. (2020), Enhancement of optical and mechanical properties of sodium silicate glasses using zirconia. Opt Quant Electron 52, 458. https://doi.org/10.1007/s11082-020-02575-3

[44] Dimitrov, V., & Sakka, S. (1996). Electronic oxide polarizability and optical basicity of simple oxides. I. Journal of Applied Physics, **79**(3) 1736. doi.org/10.1063/1.360962

[45] Dimitrov, V., & Komatsu, T. (2002). Classification of Simple Oxides: A Polarizability Approach. Journal of Solid-State Chemistry, **163**(1) 100. https://doi.org/10.1006/jssc.2001.9378

[46] Zhao, X., Wang, X., Lin, H., & Wang, Z. (2007). Electronic polarizability and optical basicity of lanthanide oxides. Physica B: Condensed Matter, 392(1-2), 132–136. 10.1016/j.physb.2006.11.015

[47] Duffy, J. A. (1989). A common optical basicity scale for oxide and fluoride glasses. Journal of Non-Crystalline Solids, 109(1), 35–39, https://doi.org/10.1016/0022-3093(89)90438-9

[48] Duffy, J. A., & Ingram, M. D. (1992). Comments on the application of optical basicity to glass. Journal of Non-Crystalline Solids, 144, 76–80. doi:10.1016/s0022-3093(05)80385-0

[49] Varshneya Arun K., (1994), Fundamentals of inorganic glasses, Academic Prese Limited, p.33.

[50] Xu, Y., Zhang, Y., Hou, L. et al. (2014), Preparation of CaO-Al_2O_3-SiO_2 system glass from molten blast furnace slag. Int J Miner Metall Mater 21, 169–174. https://doi.org/10.1007/s12613-014-0881-1

Figures

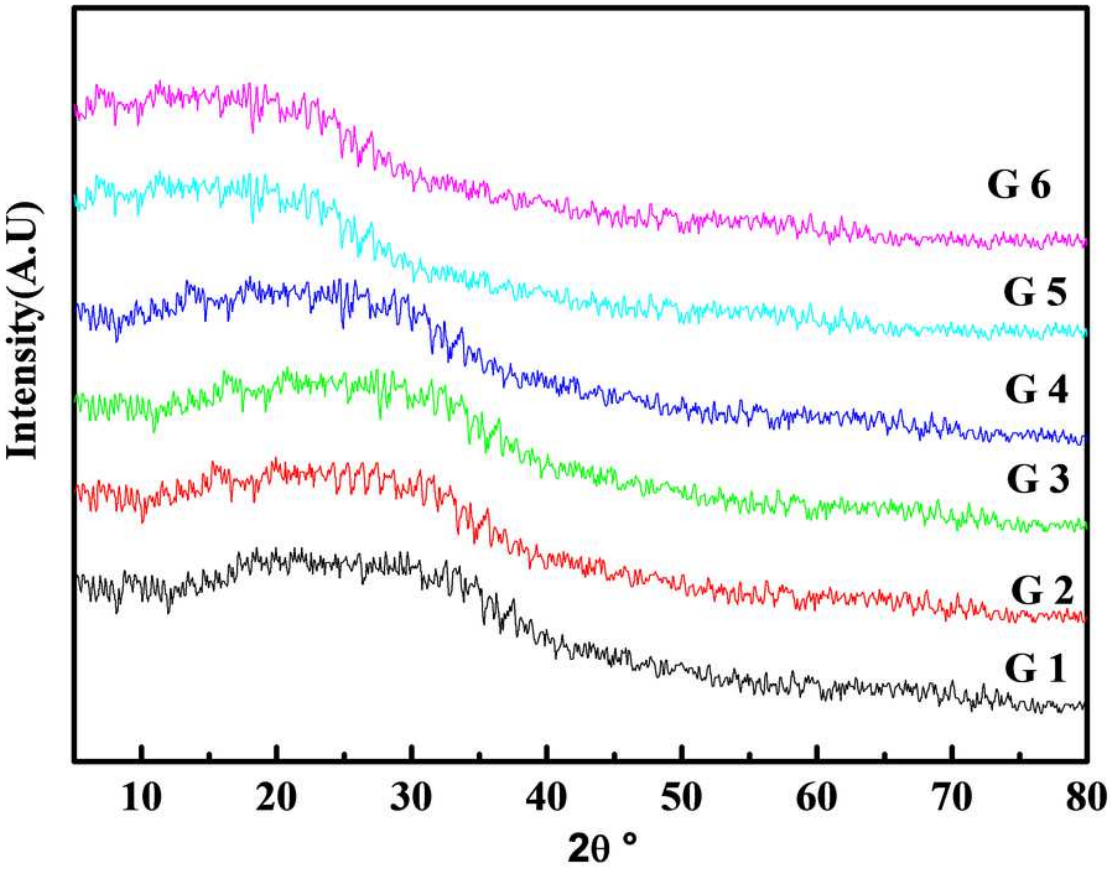

Figure 1

XRD of the studied glasses.

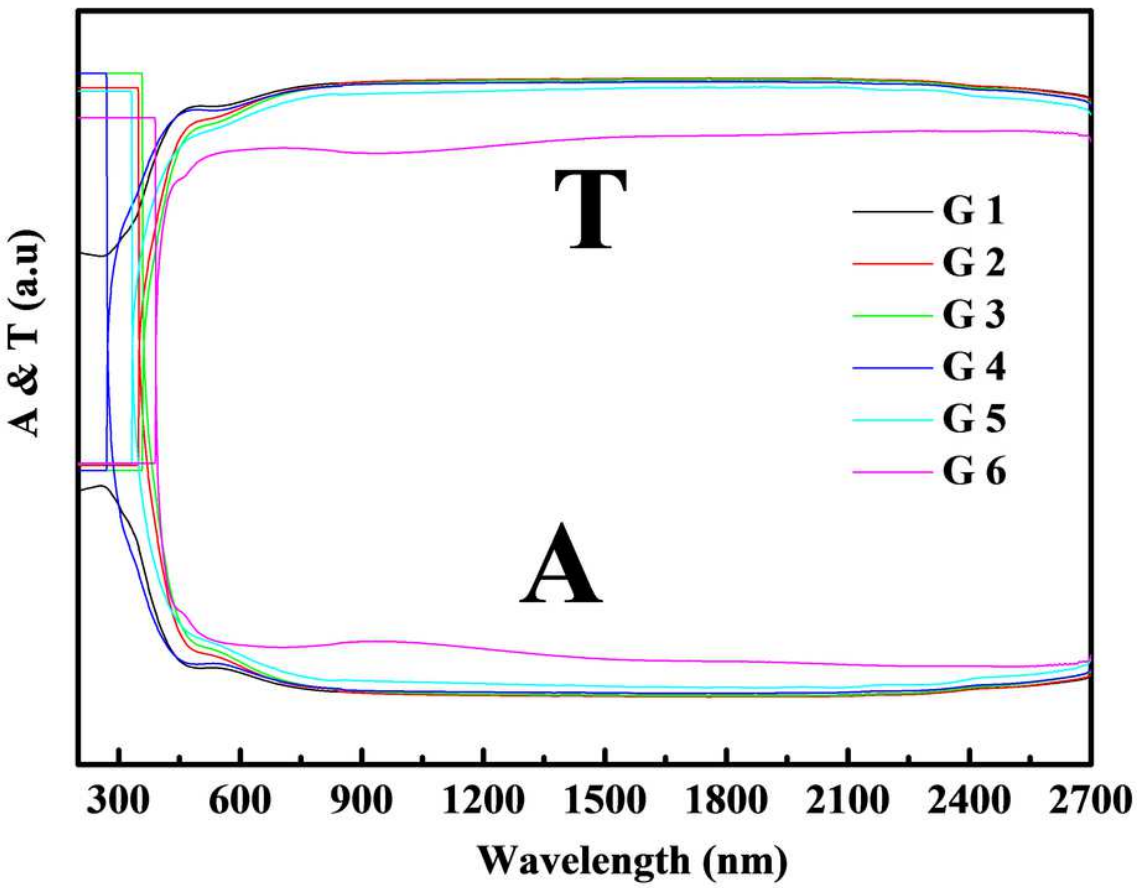

Figure 2

The absorbance (A) and transmittance (T) of the prepared glasses.

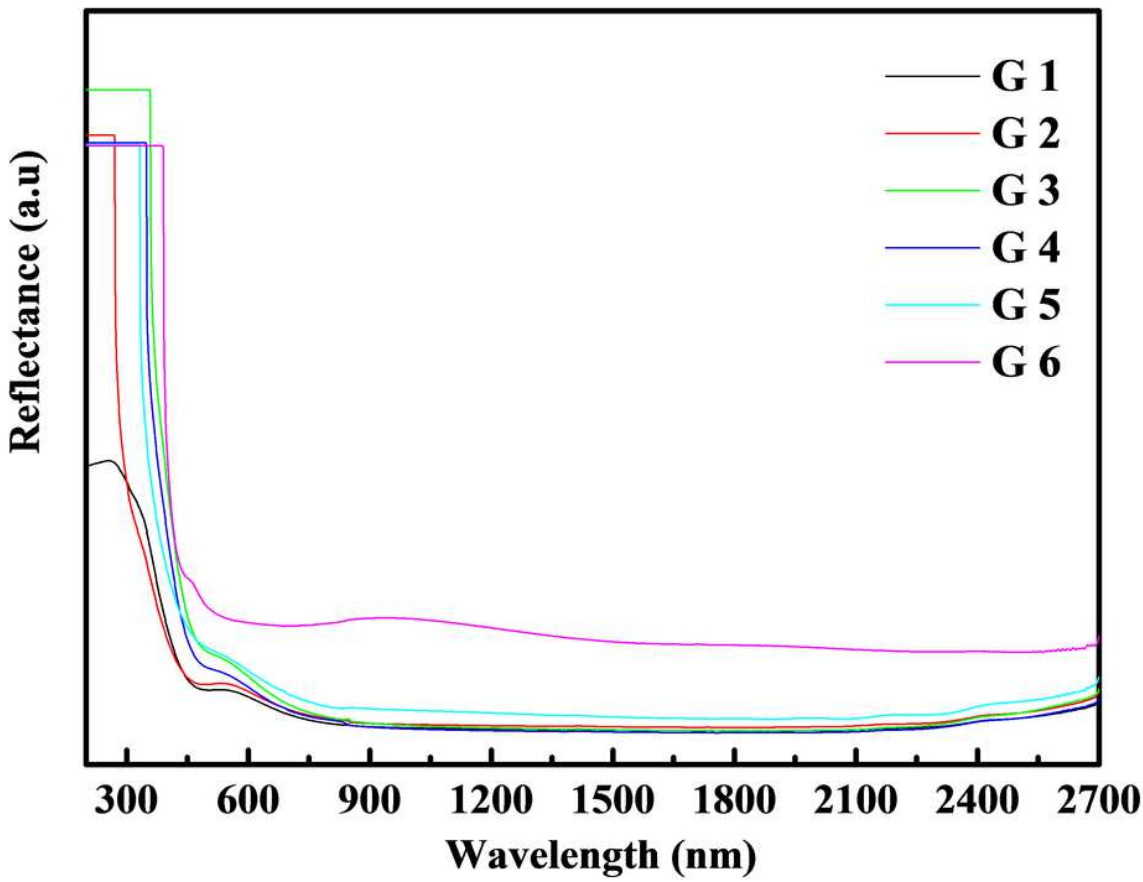

Figure 3

The reflectance (R) of the prepared glasses.

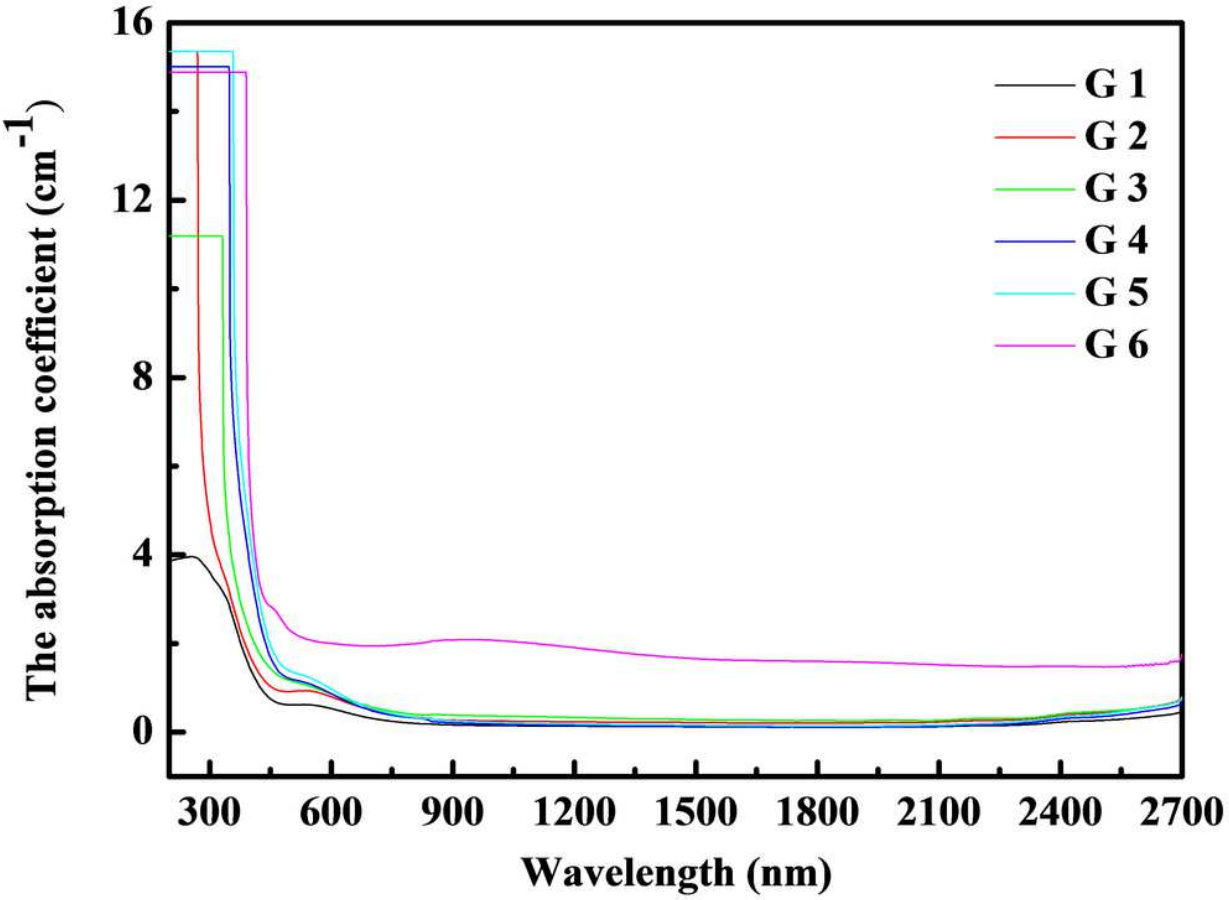

Figure 4

The absorption coefficient of the prepared glasses.

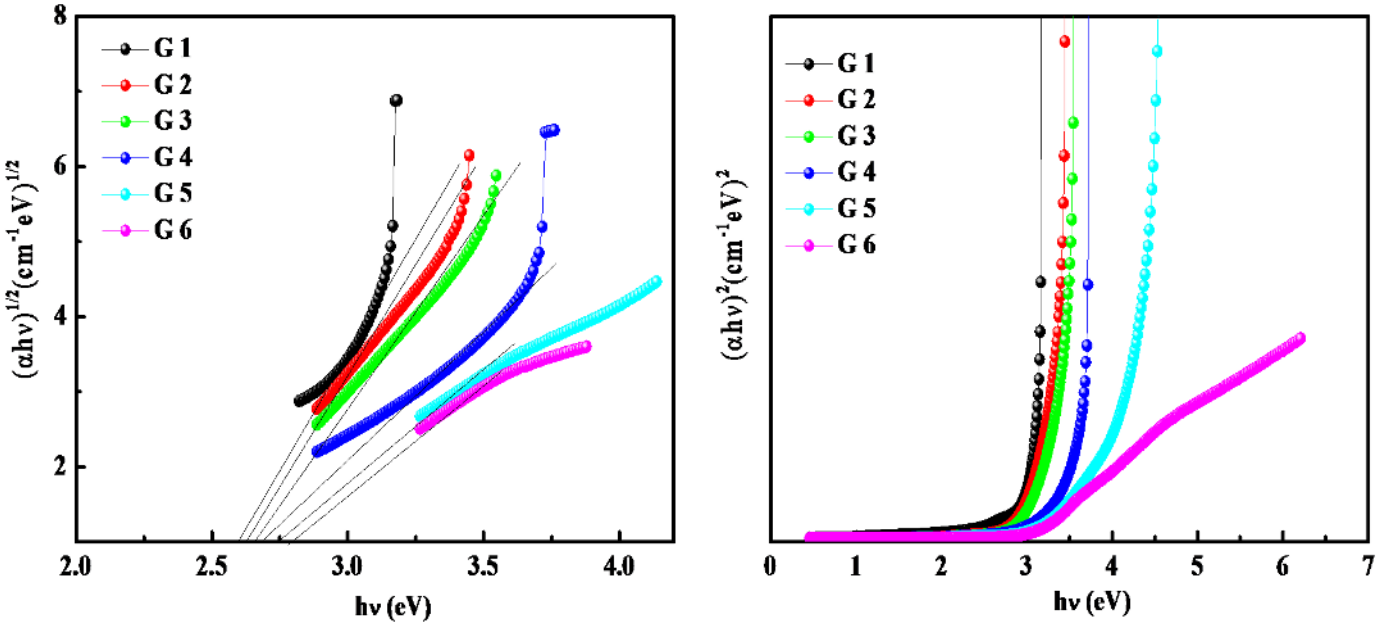

Figure 5

Plot of (α hν)1/2 and (α hν)2 against photon energy (hν) to calculate the optical band gap from the intercept of the curves.

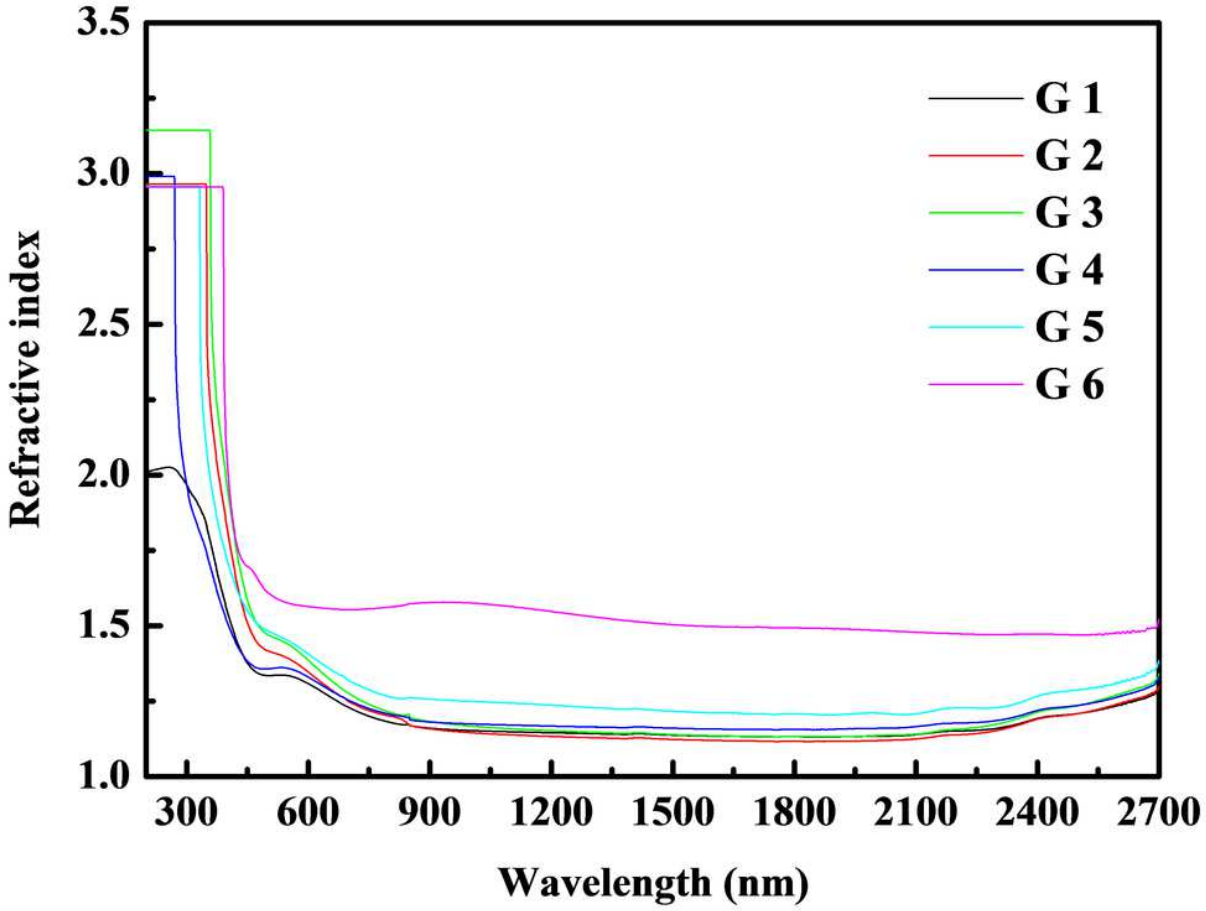

Figure 6

Refractive index of the prepared glasses.

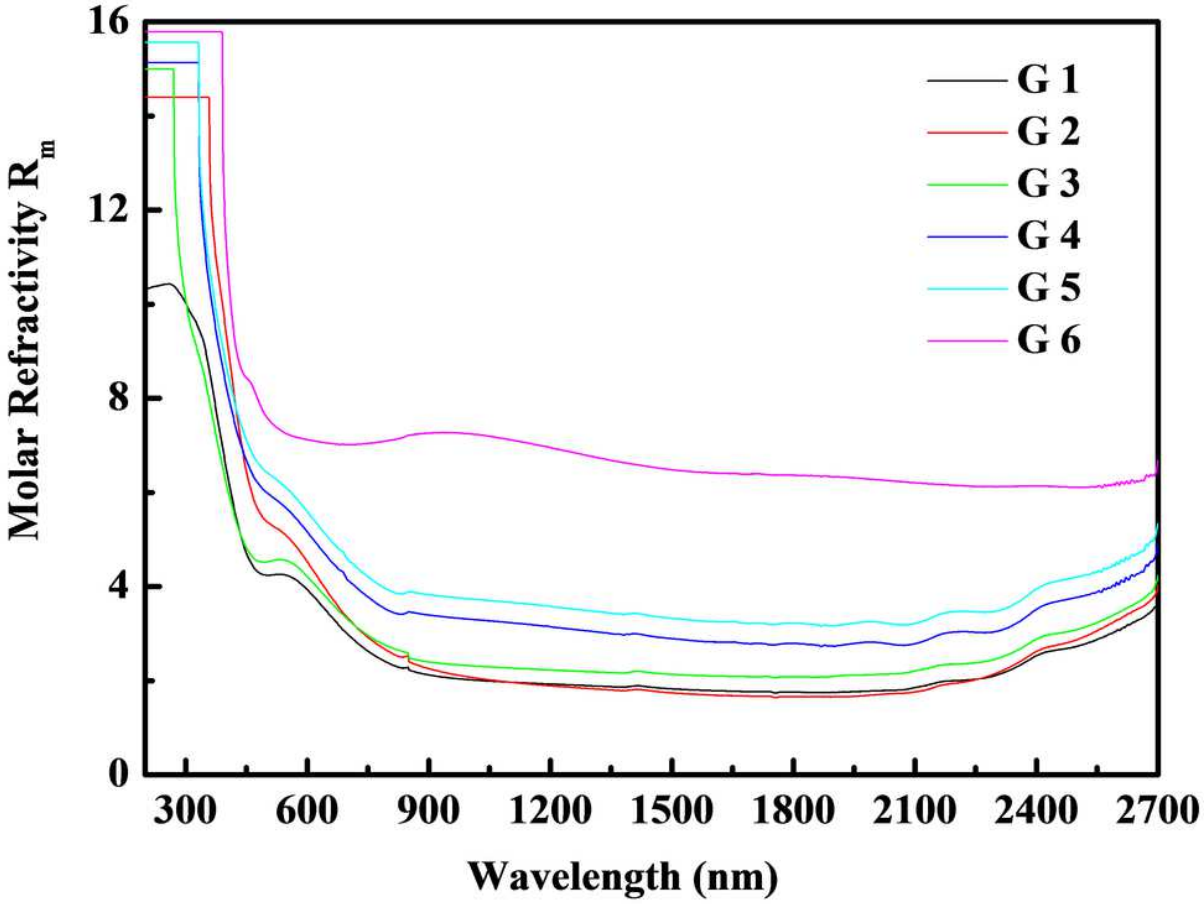

Figure 7

Molar refractivity of the prepared glasses.

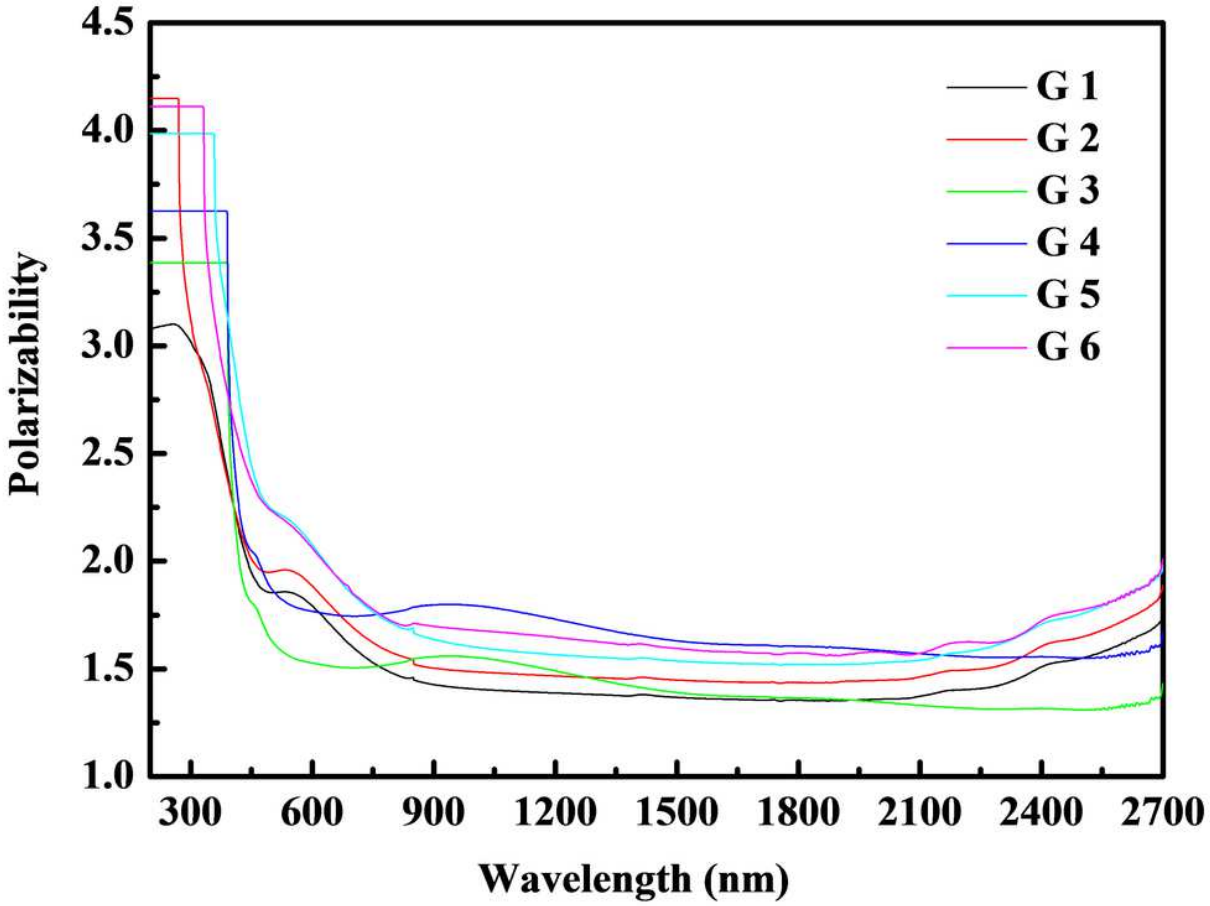

Figure 8

Electronic polarizability of the prepared glasses.

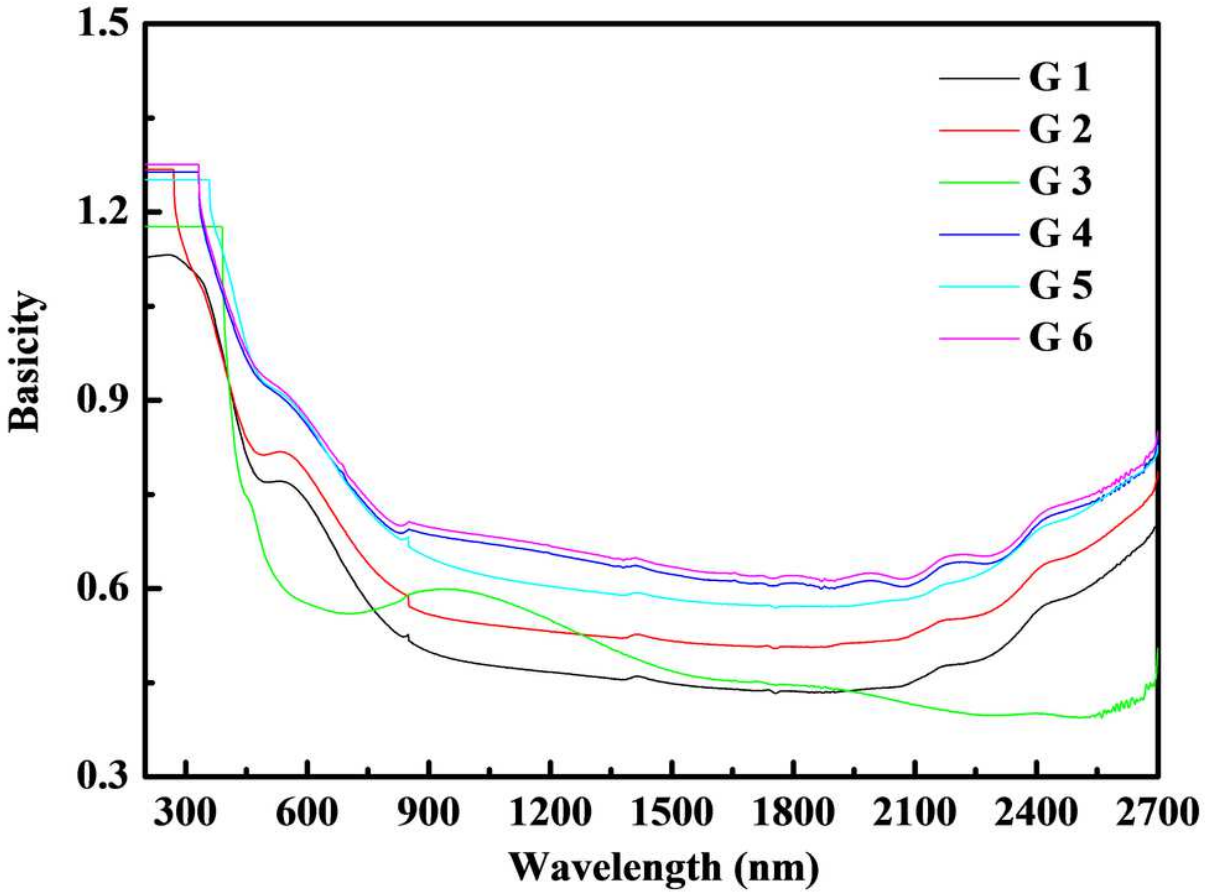

Figure 9

Optical basicity of the prepared glasses.

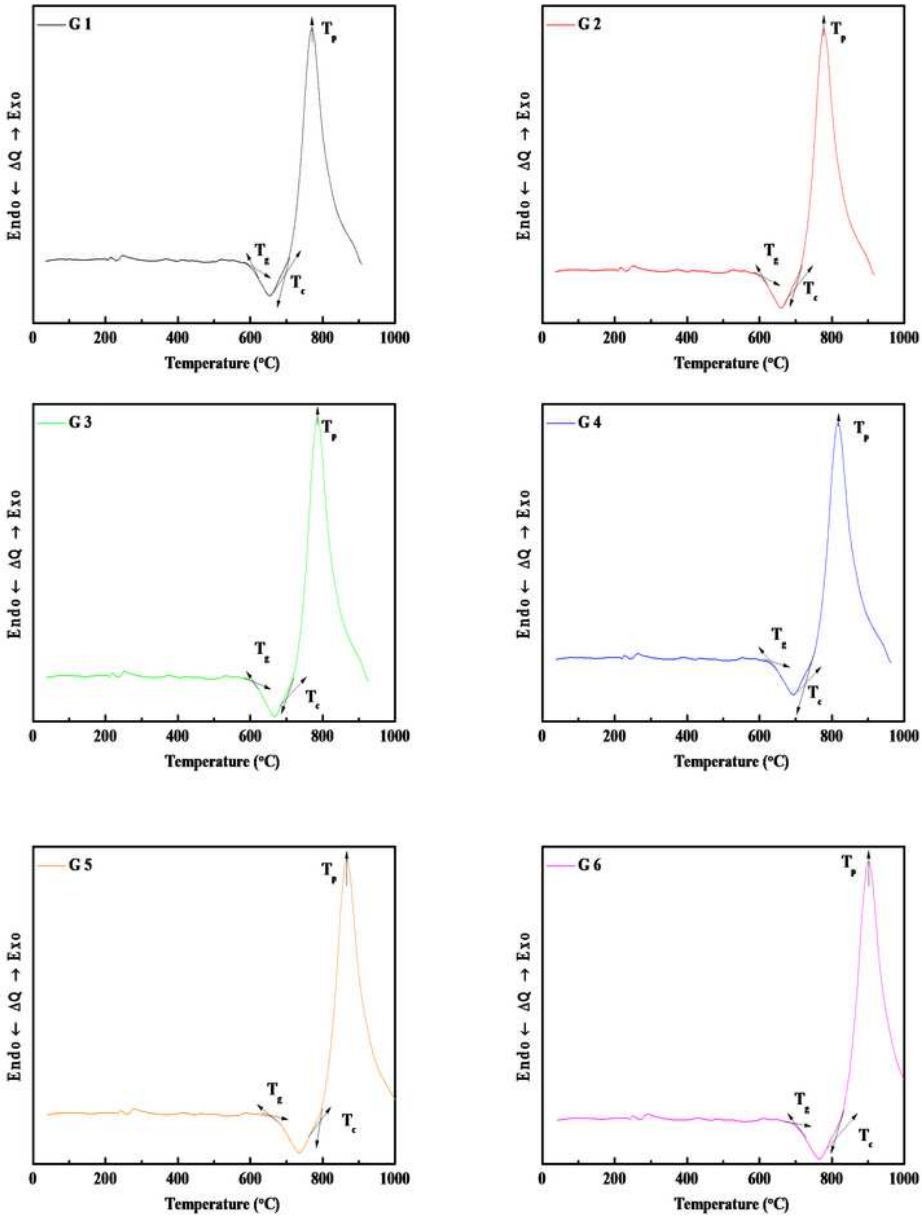

Figure 10

The DTA curves of the prepared glasses.

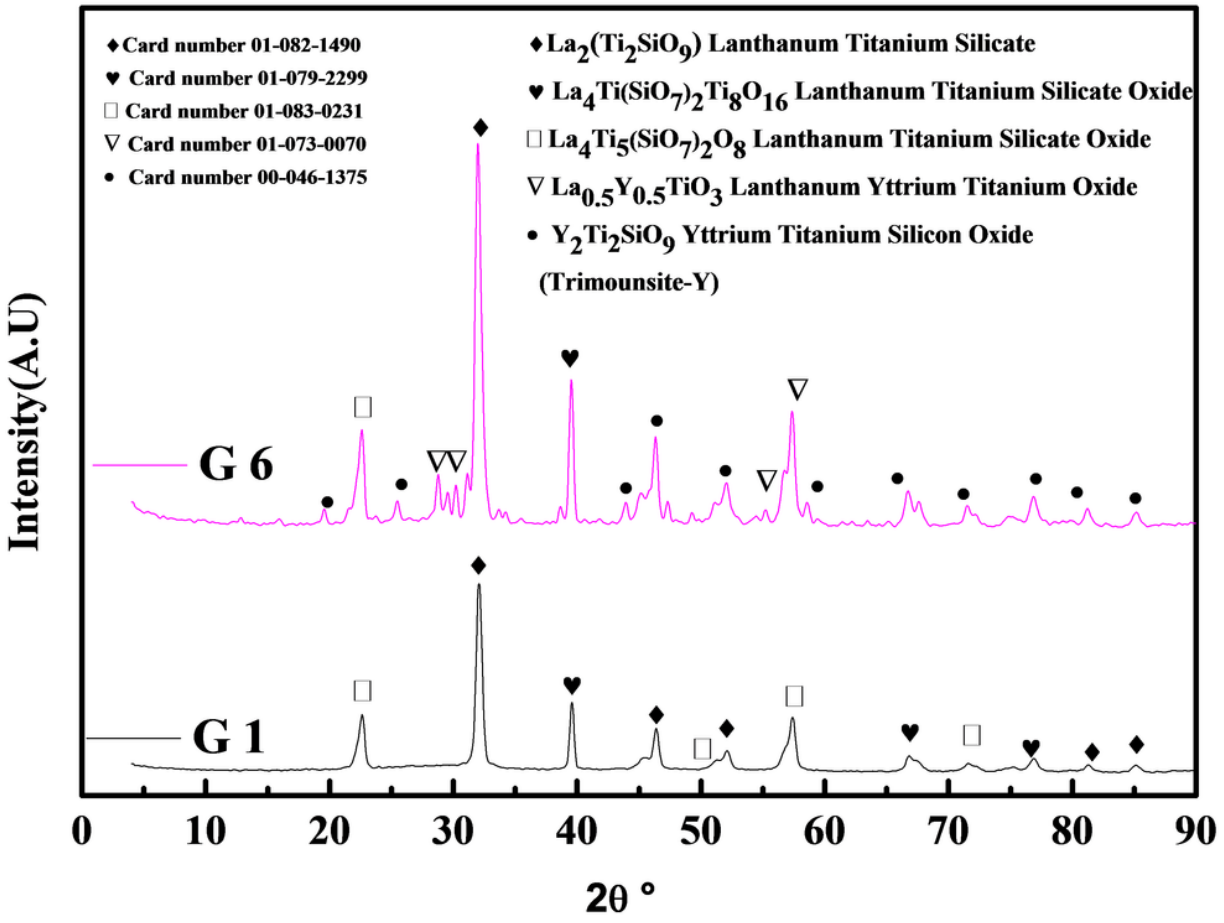

Figure 11

The XRD of the selected glass-ceramics.

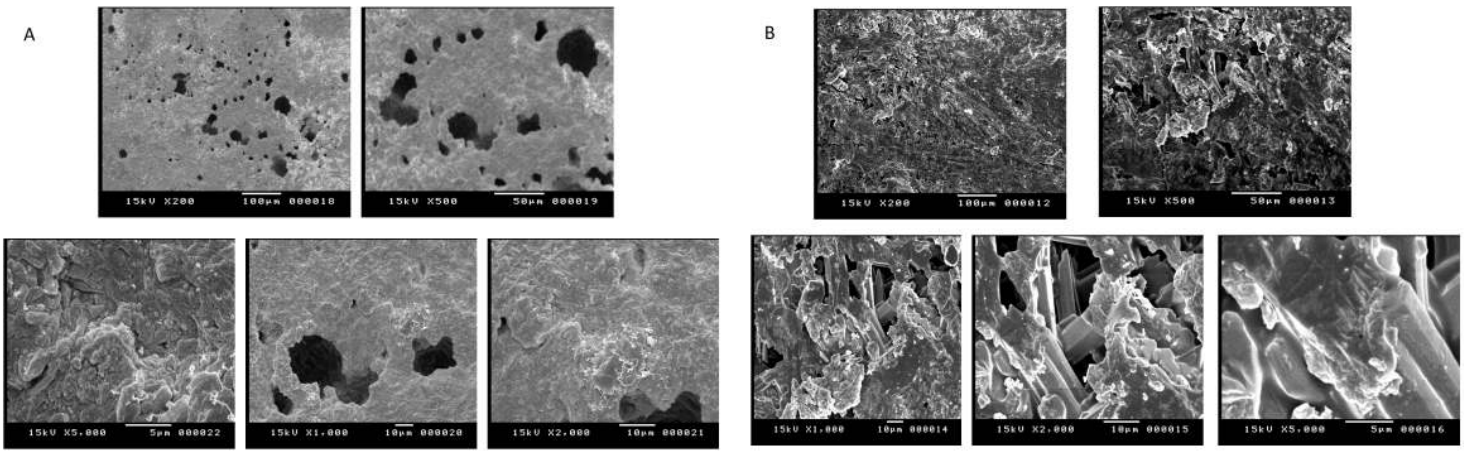

Figure 12

A: SEM backscattered electron images of the produced glass-ceramics (G 1) B: SEM backscattered electron images of the produced glass ceramics (G 6)

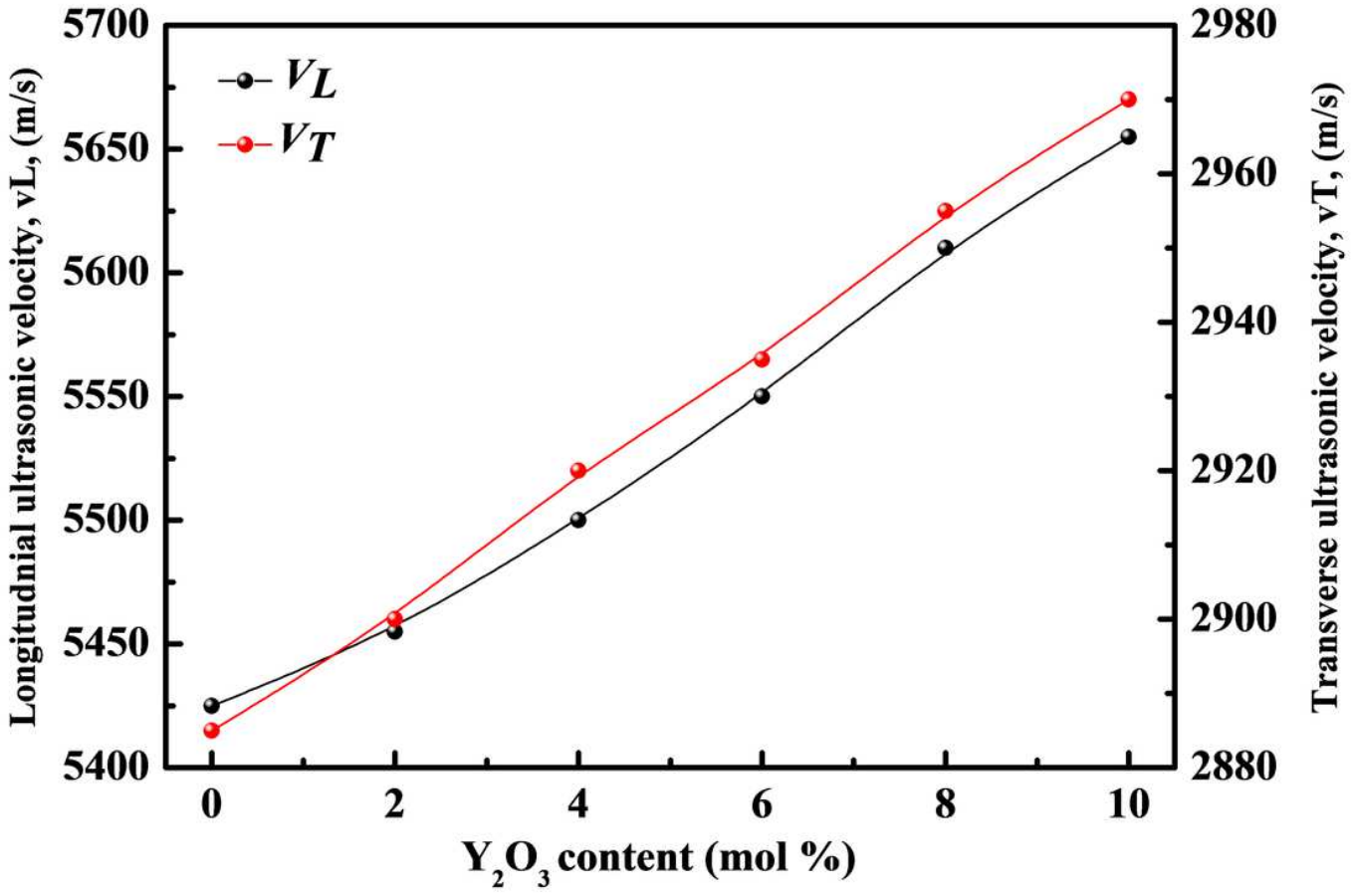

Figure 13

Dependence of the longitudinal and shear ultrasonic velocities vL and vT of the investigated glass-ceramics against of Y2O3 by mol. %.

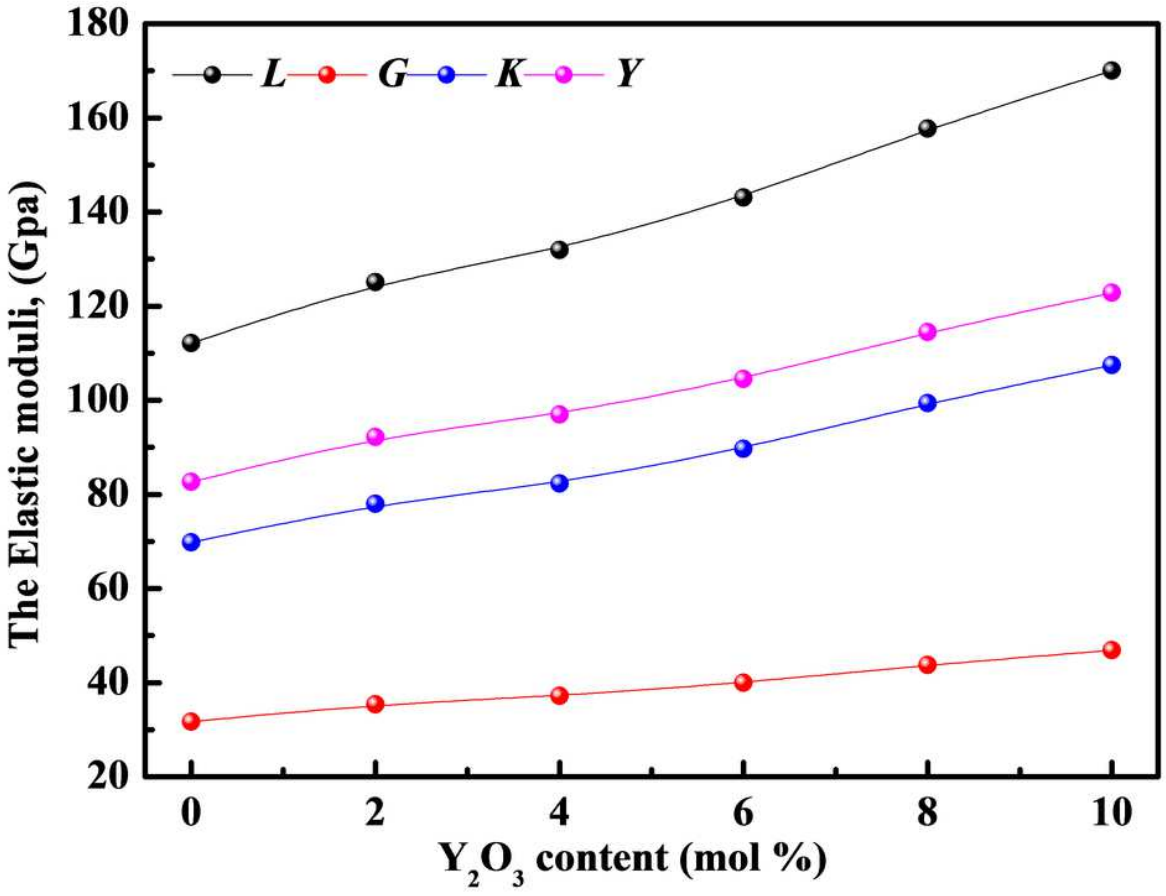

Figure 14

Composition dependence of the elastic modulus measured of the studied glass-ceramics against of Y2O3 by mol. %.